

# The Best Linear Approximation of MIMO systems: First results on simplified nonlinearity assessment

Péter Zoltán Csurscia<sup>1,2</sup>, Bart Peeters<sup>1</sup>, and Johan Schoukens<sup>2</sup>

<sup>1</sup> Siemens Industry Software NV.,  
Interleuvenlaan 68, B-3001 Leuven, Belgium

<sup>2</sup> Department of Engineering Technology (INDI)  
Vrije Universiteit Brussel  
Pleinlaan 2, B-1050 Elsene, Belgium

## ABSTRACT

Many mechanical structures are nonlinear and there is no unique solution for modeling nonlinear systems. When a single-input, single-output system is excited by special signals, it is easily possible to decide whether the linear framework is still accurate enough to be used, or a nonlinear framework must be used. However, for multiple-input, multiple-output (MIMO) systems, the design of experiment is not a trivial question since the input and output channels are not mutually independent. This paper shows the first results of an ongoing research project and it addresses the questions related to the user-friendly processing of MIMO measurements with respect to the design of experiment and the analysis of the measured data.

When the proposed framework is used, it is easily possible a) to decide, if the underlying system is linear or not, b) to decide if the linear framework is still accurate (safe) enough to be used, and c) to tell the unexperienced user how much it can be gained using an advanced nonlinear framework. The proposed nonparametric industrial framework is illustrated on a on the ground vibration testing of an electrical airplane.

**Keywords:** MIMO systems, nonlinearity, nonparametric estimation, system identification, ground vibration testing

## 1. INTRODUCTION

In this paper we focus on nonparametric vibration analysis. Many mechanical and civil structures are inherently nonlinear. The problem lies in the fact that there are many different types of nonlinear systems, each of them behaves differently, therefore modelling is very involved, and universally usable design and modelling tools are not available. For these reasons the nonlinear systems are often approximated with linear systems, because its theory is user friendly and well understood.

Since the development of advanced digital signal processing algorithms and the increased computational capability, it became possible to use complex input signals such that a large variety of shaker excitation signals can be used to experimentally determine the broadband FRFs, which are required to obtain parametric models (e.g. resonance frequencies, modes shapes, etc.). One of the (best) possibilities is the usage of special multisines (known as pseudo random signal as well) because they can avoid spectral leakage, inconsistency, non-persistence, and they provide a handy, robust solution to build linear models (FRFs) and to detect the level and type of nonlinearities. The state-of-the-art knowledge known as the Best Linear Approximation (BLA) (best in mean square error sense) framework is already available for single-input, single-output (SISO) systems [1] [2] [3] [4].

The aim of the paper is to introduce the BLA framework of multiple input-multiple output (MIMO) systems based on industrial vibrational measurements. The proposed BLA provides a user-friendly interpretation of the measurement data by extracting the user relevant information. The procedure consists of two main steps.

In the design of experiment step (step 1), systems are excited by multisine signals. The excitation signal consists of independent series of periodic multisines where each excitation channel and each experiment are mutually independent.

The analysis of the measured signals (step 2) differs from the classical H1 Frequency Response Function (FRF) estimation process. The key idea is to make use of some statistical properties of the excitation signal such that it becomes possible to split up the classical coherence function of the FRF measurement into noise and nonlinearity information.

The proposed nonparametric industrial framework is illustrated on the ground vibration testing (GVT) measurement of a battery operated electrical airplane.

This paper is organized as follows. Section 2 briefly describes the considered systems and assumptions applied in this work. Section 3 addresses questions related to the experiment design. Section 4 discusses the estimation framework in detail. In Section 5 and 6 the description of the GVT measurement and its analysis are given. Conclusions can be found in Section 7.

## 2. BASICS

The dynamics of a linear MIMO system can be nonparametrically characterised in frequency domain by its Frequency Response Matrix (FRM) [5]  $G$  at discrete frequency index  $k$ , which relates the inputs  $U$  to outputs  $Y$  as follows:

$$Y(k) = G(k)U(k) \quad (1)$$

In this work arbitrary number of input and output channels are considered and the underlying systems are BIBO stable physical systems [6]. For the sake of simplicity, the frequency indices will be omitted, and it is assumed to understand each quantity at frequency index  $k$ .

This system represented by the  $G$  is linear when the superposition principle is satisfied in steady-state, i.e.:

$$Y = G(a + b)U = a GU + b GU = (a + b) GU \quad (2)$$

where  $a$  and  $b$  are scalar values. If  $G$  is constant, for any  $a$ ,  $b$  (and excitation), then the system is called linear-time invariant (LTI). On the other hand, when  $G$  varies with  $a$  and  $b$  (and the variation depends also on the excitation signal – e.g. level of excitation, distribution, etc.) then the system is called nonlinear.

Because time-varying systems are often misinterpreted as nonlinear systems, it is important to mention that when  $G$  varies over the measurement time, but at each time instant the principle of superposition is satisfied, then the system is called linear time-varying (LTV) [7].

In this work we consider nonlinear time-invariant stable (damped) mechanical (vibrating) systems where the linear response of the system is still present and the output of the underlying system has the same period as the excitation signal (i.e. the system has PISPO behaviour: period in, same period out [8]).

Further, it is assumed that the excitation signal is known (measured precisely). The actuator of the system is linear.

## 3. DESIGN OF EXPERIMENT

### Multisine excitation and detection of nonlinearities

In modern system identification special excitation signals are available to assess the underlying systems in a user-friendly, time efficient way [9]. To avoid any spectrum leakage, to reach full nonparametric characterization of the noise, and to be able to detect nonlinearities, a periodic signal is needed. Many users prefer noise excitations, because they are simple to implement, but in this case nonlinearities are not identifiable, and there is a possible leakage error. The best signal that satisfies the desired properties is the user-friendly multisine signal (see Figure 1) which looks like Gaussian white noise, behaves like it but it is not a noise. The random phase (uniformly distributed) multisine is a sum of harmonically related sinusoids. The amplitude distribution of a random phase multisine is approximately normal (it approaches a Gaussian distribution as the number of harmonics tend to infinity).

In this work, random phase multisines are used and generated in the frequency domain such that the magnitude characteristic is set by the user, and the phases of the cosines are chosen randomly from a uniformly distribution [8]. Note that this signal is also known as pseudo-random (multisine) signal.

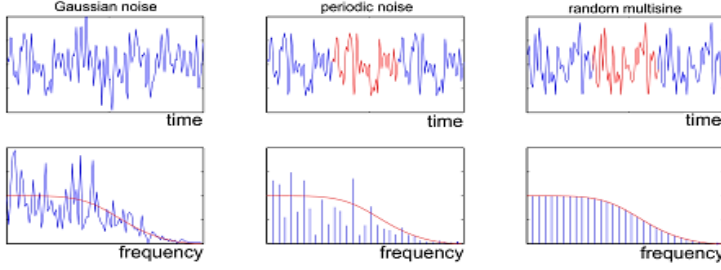


Figure 1: Different excitation signals in time and in frequency domain

### Multisines for multiple input measurements

For the sake of simplicity – without loss of generality – we will focus on systems with two inputs and two outputs. This allows to illustrate the additional problems that appear when moving from SISO to MIMO for a minimal increase of the complexity. The straightforward extension of the SISO excitation case can be formulated in frequency domain as follows:

$$Y = GU \Leftrightarrow \begin{bmatrix} Y_1 \\ Y_2 \end{bmatrix} = \begin{bmatrix} G_{11} & G_{12} \\ G_{21} & G_{22} \end{bmatrix} \begin{bmatrix} U_1 \\ U_2 \end{bmatrix} \quad (3)$$

where the indices of the input and output data refer to channel number.

The above-mentioned set of linear equations suffers from the degrees of freedom: there are 4 unknown parameters and only 2 independent equations. In order to overcome the issue with the degrees of freedom, then number of independent equations has to be increased. In this work this has been done by increasing the number of experiments by expanding the number of columns in  $U$  (and hence the number of columns in  $Y$ ). Each column in  $U$  ( $Y$ ) represents an experiment. In case of 2 inputs there are at least 2 experiments needed.

The solvability of the above-mentioned linear algebraic equation strongly depends on the condition number (i.e. the randomness) of the excitation signal's matrix  $U$ . In classical MIMO identification, one of the most often applied solution to this problem is the use of Hadamard decorrelation technique: a square matrix (whose entries are either +1 or -1) is elementwise multiplied with one realization of signal. The restriction here is that the order of the matrix must be 1, 2, or multiples of 4.

In order to overcome the issue with the limited possible orders of Hadamard matrix and to improve the estimation properties [10] and [11] proposed to use orthogonal random multisines, extending the idea of the orthogonal inputs proposed for linear MIMO measurements in [12]. In this work the proposed procedure is to generate independent random excitation for every input channel such that we have (more) randomness in the measurement with respect to the Hadamard's technique. This sequence of signals will be placed in the first blocks of experiments (i.e. first column of  $U$ ) and they will be shifted orthogonally for the subsequent experiments (i.e. the next columns in  $U$ ) with the following weighting-shifting matrix:

$$W_{cn} = e^{-j2\pi(c-1)(n-1)/N_{input}} \quad (4)$$

where  $c$  refers to input channel number (i.e. the row number in  $U$ ),  $n$  refers to the experiment number (column number in  $U$ ), and  $N_{input}$  stands for the number of inputs. In case of 2 input/output channels, for one set of realization of the multisine signal, the following equation is given:

$$\begin{bmatrix} Y_{11} & Y_{12} \\ Y_{21} & Y_{22} \end{bmatrix} = \begin{bmatrix} G_{11} & G_{12} \\ G_{21} & G_{22} \end{bmatrix} \begin{bmatrix} U_{11} & U_{12} \\ U_{21} & U_{22} \end{bmatrix} = \begin{bmatrix} G_{11} & G_{12} \\ G_{21} & G_{22} \end{bmatrix} \begin{bmatrix} U_1 W_{11} & U_1 W_{12} \\ U_2 W_{21} & U_2 W_{22} \end{bmatrix} = \begin{bmatrix} G_{11} & G_{12} \\ G_{21} & G_{22} \end{bmatrix} \begin{bmatrix} U_1 & U_1 \\ U_2 & \bar{U}_2 \end{bmatrix} \quad (5)$$

#### 4. BEST LINEAR APPROXIMATION

The Best Linear Approximation (BLA) has been widely used in the last decades to efficiently estimate FRFs [9]. The BLA of a nonlinear system is an approach of modelling that minimizes the mean square error between the true output of a nonlinear system and the output of the linear model.

The proposed BLA technique makes use of the knowledge that the excitation signal has both stochastic and deterministic properties. In this work the excitation signal is random phase multisine signal and it is assumed to be measured precisely. In each measurement there are  $m$  different random realizations of multisines (orthogonally shifted number of input channels times) and each of the realization is repeated  $p$  times.

From the philosophical point of view there are two main differences between the proposed BLA and the classical H1 (cross-power spectral density) estimate [13] frameworks. First, in the BLA case the FRM is estimated from the discrete Fourier transformed data instead of using the cross-power and auto-power matrices. Second, instead of directly using the averaged input and output data, a partial BLA estimate is calculated for each period of the excitation. A BLA FRM estimate, for a given signal, is then calculated via the average of partial BLA estimates. In this case we can easily estimate the noise levels and standard deviations on each frequency line. Using this information, the coherence function will be virtually split into (1) noise level and (2) nonlinear contribution estimates.

#### Theoretical structure and the basic assumptions

As aforementioned, the BLA of a nonlinear system is an approach of modelling that minimizes the mean square error between the true output of a nonlinear system and the output of the linear model [8]. In the proposed robust BLA framework, multiple repeated realizations of random phase multisine excitation are needed. The BLA estimate consists of several components. Figure 6. Shows the theoretical structure of the considered BLA estimator.

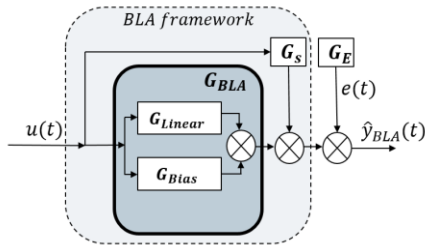


Figure 2: The theoretical structure of the best linear approximation

$G_{Linear}$  is the linear (transfer function) component of BLA. This component is phase coherent: random phase rotation in the input excitation would result in a proportional phase rotation at the output.

In case of non-coherent behaviour, the input phase rotation would result in a random phase rotation at the output. Please note that significant part of the nonlinearities is non-coherent. When many input phase rotations are performed, the random output rotations can be seen as an additional (nonlinear) noise source ( $G_S$ ) next to the ordinary measurement noise ( $G_E$ ) – assumed to be additive i.i.d. normal distributed with zero mean with a finite variance. The usage of periodic excitation reduces the effects of the measurement noise  $G_E$ . The usage of multiple random phase realizations reduces the level of non-coherent nonlinearities.

The (coherent) nonlinearities remaining after multiple realizations of excitation signal result in a bias error of the BLA (denoted by  $G_{Bias}$ ). The next section discusses a possibility to reduce the effects of  $G_S, G_E$ .

#### Two-dimensional averaging

When the BLA estimation framework is applied, the observed system is excited by random phase multisines (assumed to be measured precisely). In this work there are ( $N_{input}$  times phase-rotated)  $m$  different realization of the multisine excitation signal, each realization is repeated  $p$  period times. The considered steady-state model in frequency domain at frequency bin index  $k$  is given by:

$$\hat{G}^{[m][p]} = \hat{Y}_{measured}^{[m][p]} U^{[m]-1} = \hat{G}_{BLA} + \hat{G}_S^{[m]} + \hat{G}_E^{[m][p]} \quad (3)$$

The steady state signals are obtained in this work by discarding some periods at the beginning of each realization block. In order to estimate the underlying system one has to average over  $p$  periods of repeated excitation signal, and over the  $m$  different realizations of the excitation signal [8] (see Figure 3).

First, let us average over the  $p$  periods of a realization. If  $p$  is sufficiently large then (considering the law of large numbers and the distribution properties the observation noise) the expected value of  $\hat{G}_E^{[m][p]}$  converges to zero, so that term is eliminated. In other words, averaging over repeated blocks results in an improvement of the SNR. Because the stochastic nonlinear contribution  $\hat{G}_S^{[m]}$  does not vary over the repetition of the same realization we have to average over the  $m$  different realizations. If  $m$  is sufficiently large, then  $\hat{G}_S^{[m]}$  ‘half-stochastic’ nonlinear noise source converges to zero, so that term is eliminated. After the 2D averaging the BLA estimate is obtained.

The estimate of the noise sample variance  $\hat{\sigma}_{G_E}^2$  is calculated from the averaged sample variance of each FRM realization. The total variance of the FRM  $\hat{\sigma}_{G_{BLA}}^2$  is calculated from the sample variance of each different partial BLA estimates  $\hat{G}^{[m]}$ .

The difference between the total variance and the noise variance is an estimate of the variance of the stochastic nonlinear contributions  $\hat{\sigma}_{NL}^2 \approx (\hat{\sigma}_{G_{BLA}}^2 - \hat{\sigma}_{G_E}^2)$ . When the user intends to see how much nonlinearity is present on an arbitrary experiment, one has to consider  $m$ -times  $\hat{\sigma}_{NL}^2$  such that  $\hat{\sigma}_{G_S}^2 \approx m\hat{\sigma}_{NL}^2$ .

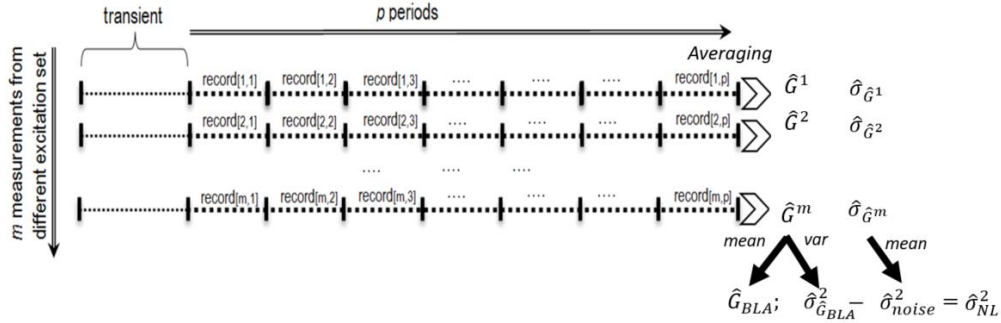


Figure 3: Evaluation of BLA estimate with the help of 2D averaging

Using the proposed 2D averaging technique the influence of the noise and nonlinear contribution can be decreased, and the final result is BLA FRF estimate. In [5] it has been suggested to choose the number of periods more than one ( $p \geq 2$ ) and the different realizations are more than six ( $m \geq 7$ ). Detailed calculations of the proposed 2D approach can be found in [14].

## 5. MEASUREMENT

This section provides a brief overview of the GVT measurement of a battery operated small aircraft. The measurement took place at Magnus testing facility in Kecskemét, Hungary in 2017. The eFusion aircraft (see Figure 4) is a two-seat, all-electric, low-wing monoplane, based on the piston engine. The light sport aircraft has a symmetric wing profile, a titanium firewall, and a centre section made of chrome molybdenum alloys. The fuselage is attached with a non-retractable tricycle landing gear. It has a length of 6.7 m, height of 2.4 m, and a wingspan of 8.3 m including winglet, whereas the wing area is 10.59 m<sup>2</sup>. The aircraft is powered by a 60kW electric drive system. The electric propulsion system including motor and batteries is designed by Siemens. The aircraft has an endurance of approximately one hour. The aircraft has an empty weight of 410 kg and a maximum take-off weight of 600kg. It requires a landing roll from 150 m to 200 m.

The measurement setup (see Figure 5) consists of 2 shakers–2 force cells, and various 91 acceleration channels. The shaker reference (Volt) signals are random phase multisine signals. The sampling frequency is 200 Hz. The period length is 1024

resulting in a frequency resolution of 0.1953 Hz. The smallest excited frequency is 1.1719 Hz, the highest excited frequency is 50.7813 Hz.

There are eight different multisine realizations for each input channel per experiment. Each multisine realization is repeated 3 times. As explained earlier, the extra experimental blocks (necessary to solve the MIMO equations) are obtained by orthogonal phase shift. Thus, there are in total  $m \cdot p \cdot N_{input} = 8 \cdot 3 \cdot 2 = 48$  blocks.



Figure 4: The eFusion battery operated small aircraft



Figure 5: The measurement setup and instrumentation.

## 6. ANALYSIS

This section concerns the analysis the random phase multisine GVT measurement. The GVT measurement has been executed at three different levels. Figure 6 shows the lowest and highest level excitation signals in the frequency domain. The excitation force is measured with approximately 65 dB SNR. This SNR is sufficiently good to fulfil the assumption on the precise excitation signal measurement. However, it is interesting to point out that the high level excitation signal is 10 dB higher than the low level excitation signal but the SNR improvement is only around 2 dB: the noise level estimate moved together with the excitation signal estimate. This indicates the presence of (low level) nonlinearities at the excitation system. The analysis of this phenomenon is out of the scope of this paper. Further, in order to simplify the analysis, the output and FRF are shown at the driving points only. The output (acceleration) measurement is shown in Figure 7. As can be seen, the SNR dropped a little resulting around 60 dB SNR at the resonances. At the higher excitation level, the right wing SNR decreased with approximately 4 dB. This is a further indication of nonlinearities being present at the measurement.

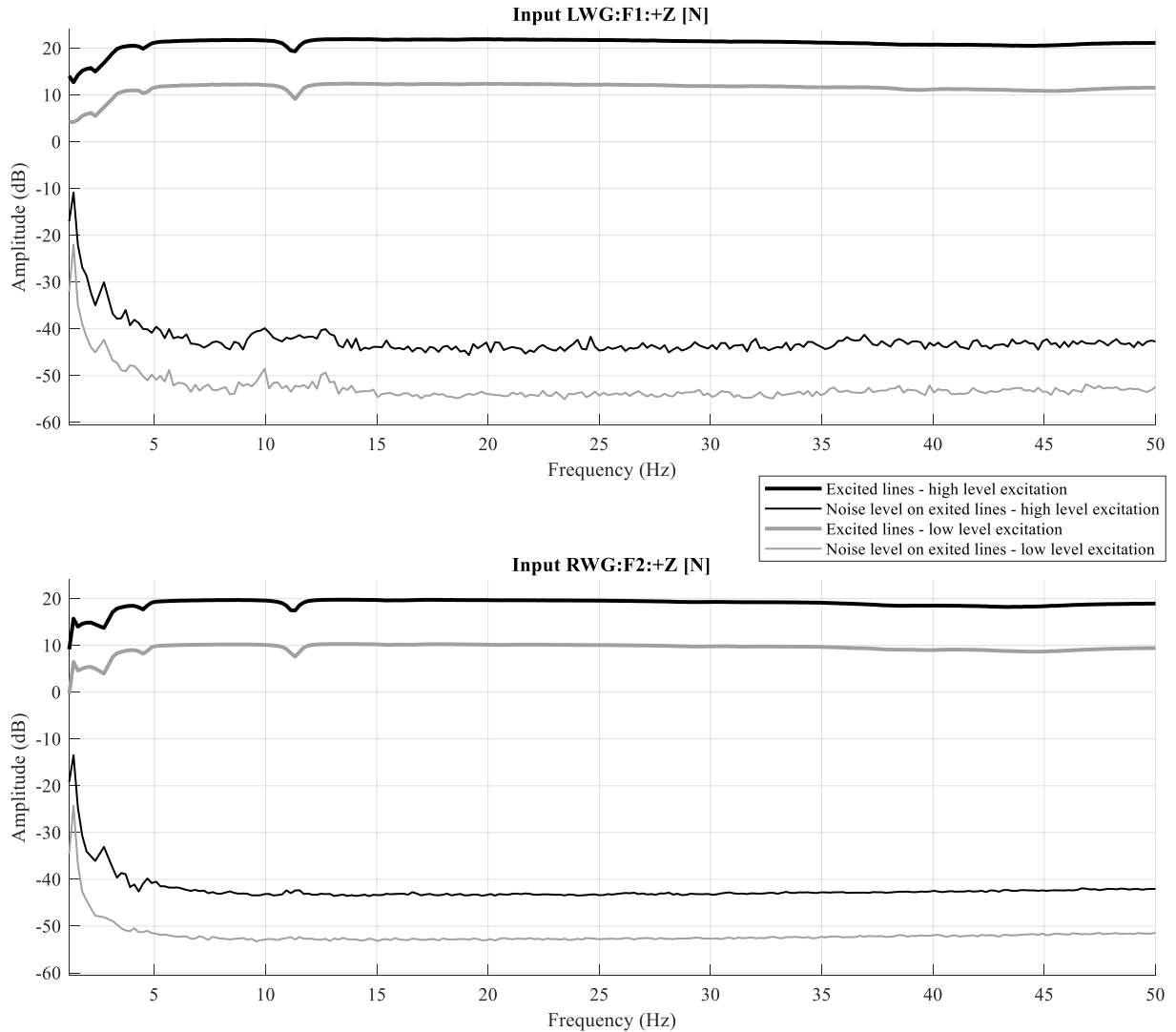


Figure 6: The input (force) signal measured in frequency domain at the low and high amplitude levels.

In order to ensure that the measured signals are in the steady-state, a simple transient check-up is performed. Figure 8 shows the first realization of one of the output channels (with the slowest decay) in time domain. In order to determine the length of the transient (i.e. the number of delay blocks), the last block (period) of the first realization – assumed to be in steady-state – is subtracted from every block in that realization. As can be seen on the right side of Figure 8, only the first block is disturbed by the transient. In this work, each first block (period) is discarded.

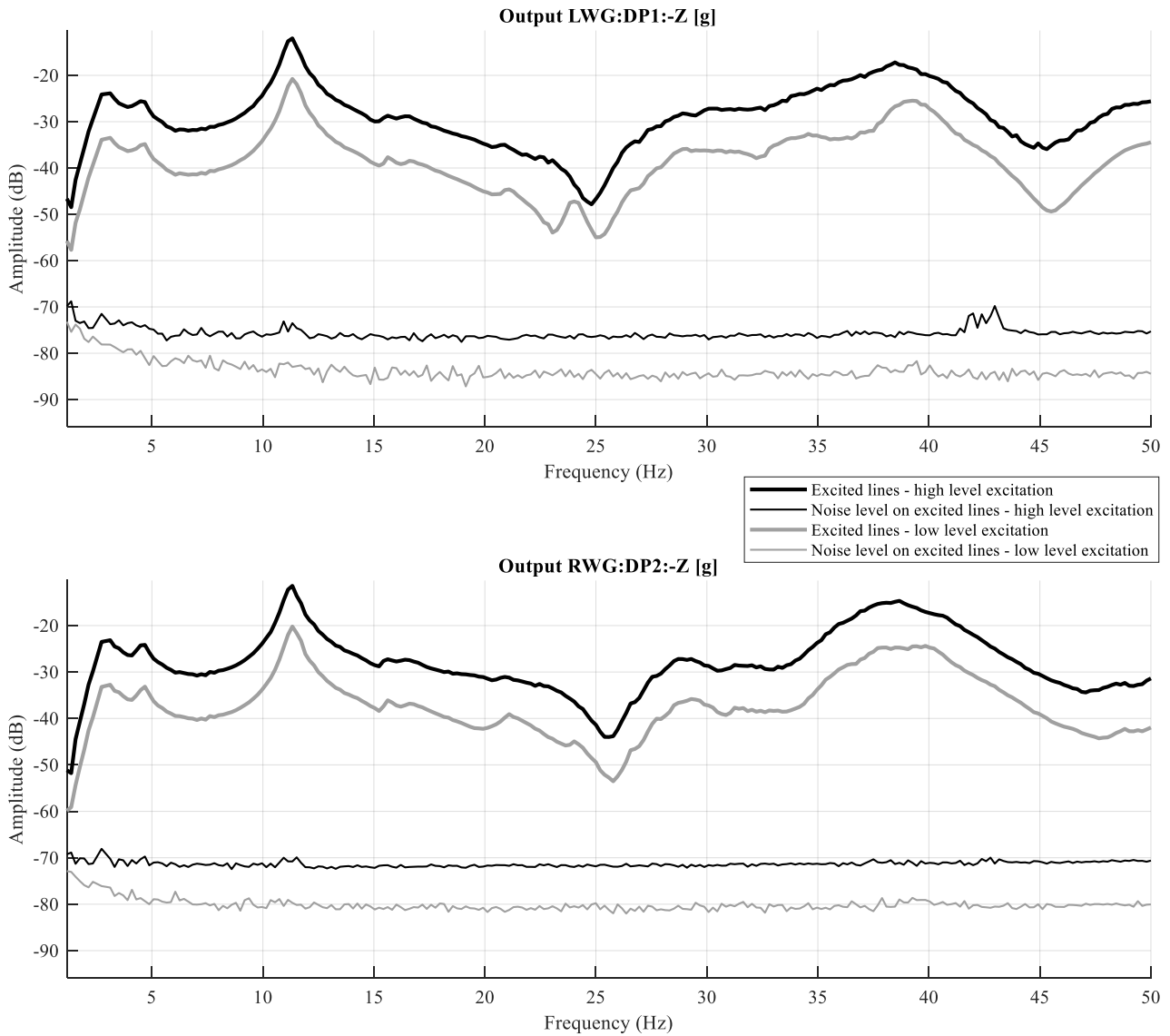


Figure 7: The output (acceleration) signal measured in frequency domain at the low and high amplitude levels.

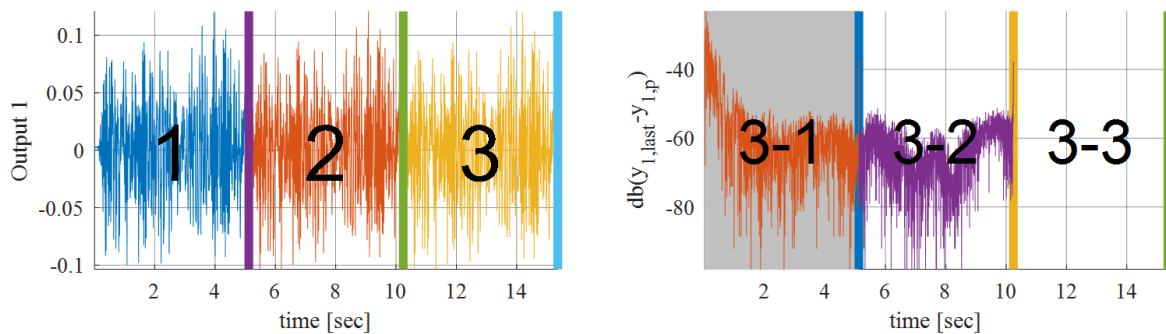


Figure 8: Periodicity of the output measurement at high level in time domain. Left figures shows the block repetitions in one realization. The right figure shows the difference between the last block minus every block.



Figure 9 shows the FRFs at the driving points at low and high level excitation. It can be clearly observed that FRFs at different levels differ a lot from each other. This clearly indicated the presence of nonlinearities. The interesting point here is to tell the inexperienced user from only one measurement if the system is linear or nonlinear – on that particular level of excitation.

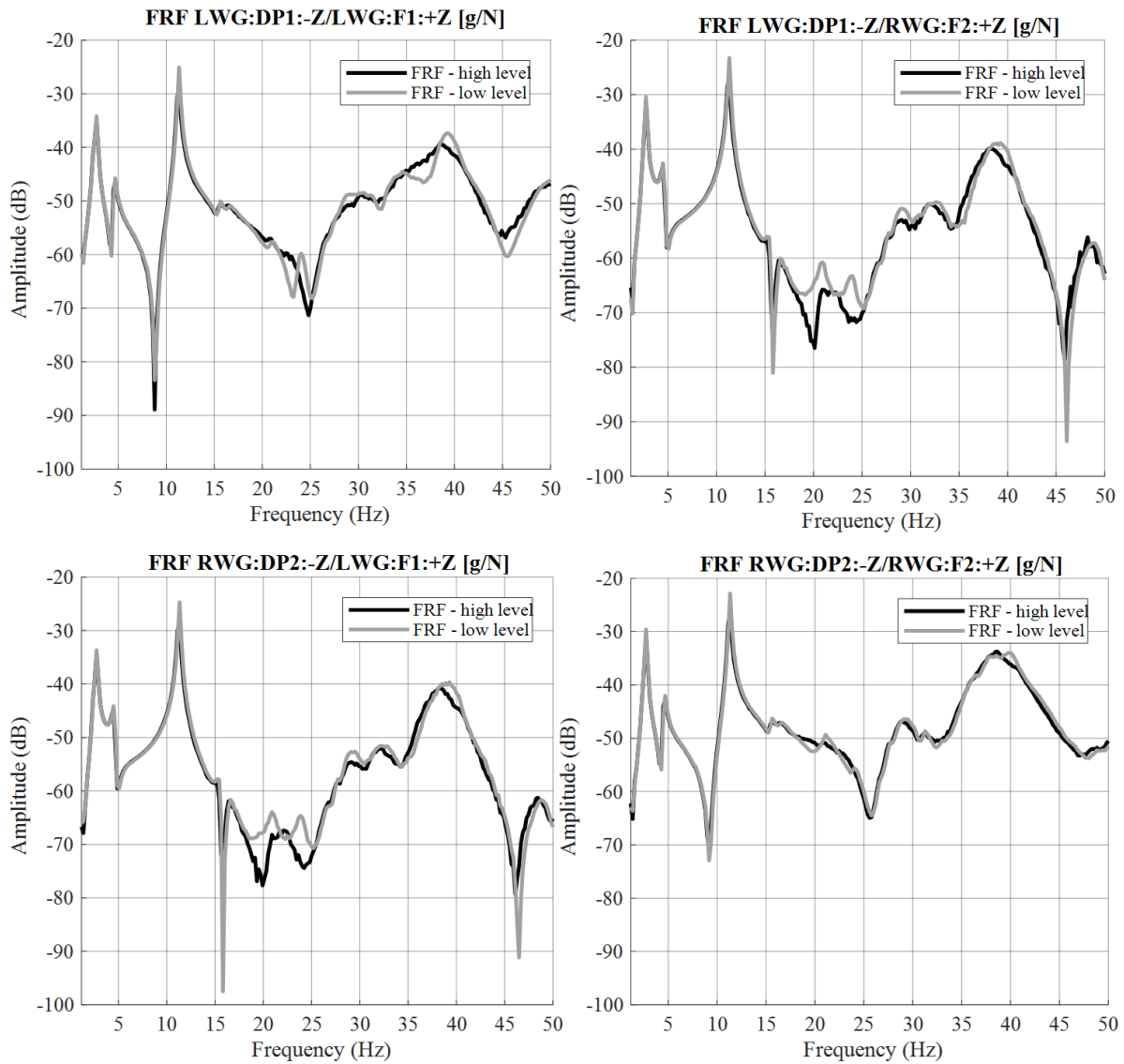


Figure 9: FRFs at driving points estimated at the low and high excitation levels.

The classical H1 framework suggest calculating the coherence function for each frequency line. When the coherence function gives one it means that there is 100% linear correlation between the measured output and input data. When the coherence is lower than one it indicates the presence of (among others) high level noise and/or transient and/or leakage and/or nonlinearities. Since we have used periodic excitation with discarding the delay blocks (transient), we made sure that the lack of coherence stands only for the noise and nonlinearities. In the following part we focus on the first FRF in FRM at high level excitation.

In the classical H1 framework the coherence function (pink thick line in Figure 10) is used to estimate the FRF measurement's standard deviation (pink thin line in Figure 10). For the numerical computation of coherence function in MIMO case we refer to [15]. Please note that by the use of the proposed BLA framework we can directly estimate the standard deviation and split it to into noise level estimation (black thin line in Figure 10) and nonlinearity level estimation (red thin line in Figure 10) as explained in the 2D averaging section of this paper.

With the help of these curves it is possible to tell how much is from the lack of coherence accounts for the noise and nonlinearity. For instance, the first resonance (around 3 Hz) has an SNR of 35 dB and an SNLR (signal-to-nonlinearity ratio) of 40 dB. This means that at this resonance the main error source is the noise. Looking at the largest resonance (4<sup>th</sup> resonance at around 12 Hz) one can read that the SNR is around 60 dB and the SNLR is around 30 dB. At this resonance the dominant error source is the nonlinearity.

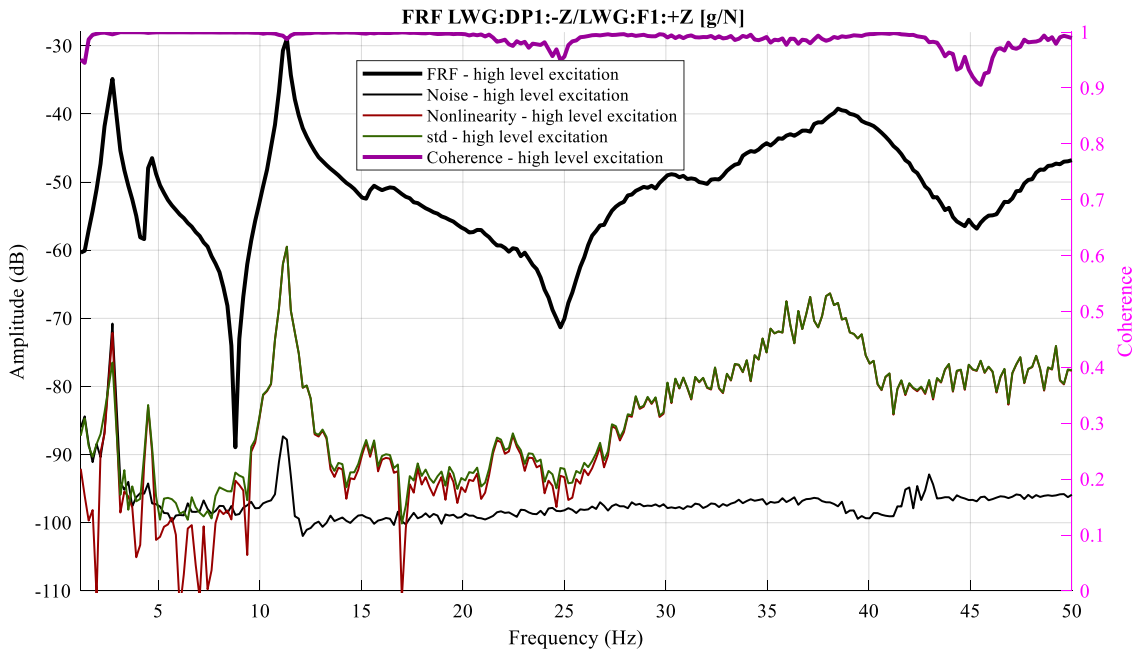


Figure 10: The BLA FRF estimation at high level excitation using the proposed technique – taking into account all data.

A further interesting point is to highlight that periodic excitation is used, therefore it is possible to estimate the standard deviation directly from the data instead. A standard deviation comparison between BLA and H1 is shown in Figure 11. This comparison indicates that the BLA estimate is indeed more robust – the BLA’s standard deviation can reach lower values than the standard deviation of H1.

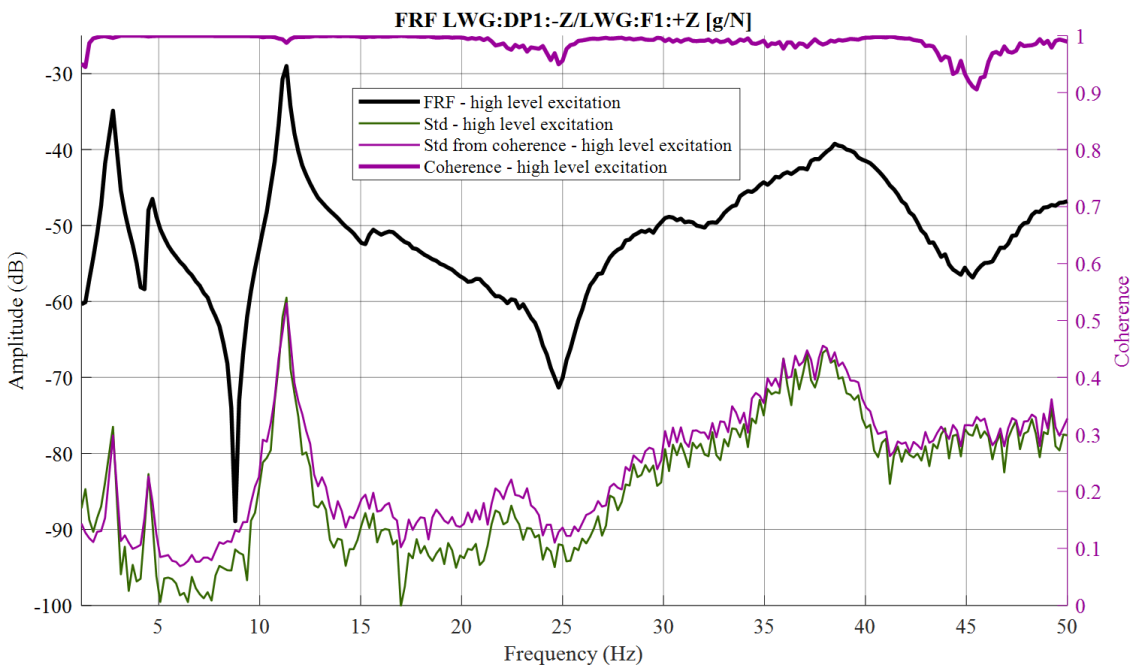


Figure 11: Comparison of standard deviation estimation of BLA estimate (green line) and H1 (pink thin line).

The figures above show the improved FRM, noise and nonlinearity estimates by taking into account all the different realizations and experiments. The question arises: what would be the noise and nonlinearity level on an arbitrary chosen measurement block (period) without using the BLA technique. In this case one has to correct for the number of experiments (multiply the noise estimate by  $\sqrt{p \cdot m}$ , nonlinearity estimates by  $\sqrt{m}$ ). This is shown in Figure 12 for both low (lighter colors) and high (darker colors) level excitation. In this case, if the end-user decides the use a simple linear model in his application the error levels would be in order of SNLR. If the end-user decides to opt for an appropriate nonlinear model the error levels would be in order of SNR. The gain (improvement) by the use of an advanced nonlinear model would be approximately the difference between the SNR and SNLR.

A further interesting thing to mention is that the anti-diagonal FRFs have a significantly higher nonlinearity level then in the diagonal FRFs.

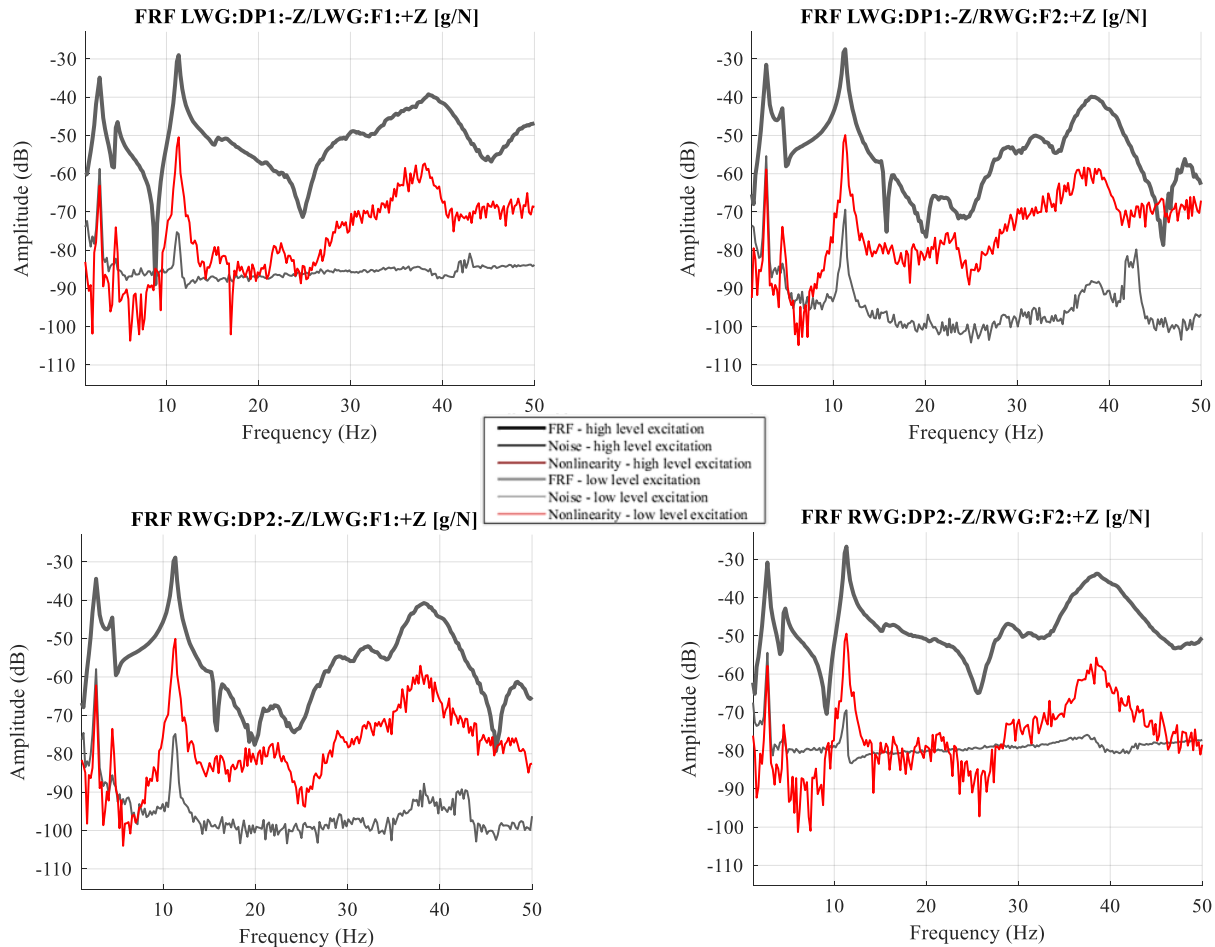


Figure 12: Expected noise and nonlinearity levels at one measurement block (period).

## 7. CONCLUSION

In this work a MIMO Best Linear Approximation framework was developed to provide a user-friendly interpretation of the nonlinear behavior of MIMO measurement data by extracting user relevant information. The proposed framework turned to be useful for modelling FRFs because:

- orthogonal excitation signals have been provided 1) to improve the SNR, 2) to better characterize the underlying system, 3) to avoid spectral leakage, and 4) to overcome the issues with transient.

- the input and output measurements were characterized,
- the frequency response matrix was estimated and characterized by virtually slitting up the coherence function into noise and nonlinearity level information
- at each amplitude level the noise and nonlinearity information can be retrieved.

Using the provided information potential users can decide if the usage of an advanced nonlinear framework is necessary.

## ACKNOWLEDGEMENTS

This work was funded by the VLAIO Innovation Mandate project number HBC.2016.0235.

## REFERENCES

- [1] L. Lauwers, J. Schoukens, R. Pintelon and M. Enqvist, "Nonlinear Structure Analysis Using the Best Linear," in *Proceedings of International Conference on Noise and Vibration Engineering*, Leuven, 2006.
- [2] A. Esfahani, J. Schoukens and L. Vanbeylen, "Using the Best Linear Approximation With Varying Excitation Signals for Nonlinear System Characterization," *IEEE Transaction on Instrumentation and Measurement*, vol. 65, pp. 1271-1280, 2016.
- [3] H. K. Wong, J. Schoukens and K. Godfrey, "Analysis of Best Linear Approximation of a Wiener–Hammerstein System for Arbitrary Amplitude Distributions," *IEEE Transactions on Instrumentation and Measurement*, vol. 61, no. 3, pp. 645-654, 2012.
- [4] J. Schoukens and R. Pintelon, "Study of the Variance of Parametric Estimates of the Best Linear Approximation of Nonlinear Systems," *IEEE Transactions on Instrumentation and Measurement*, vol. 59, no. 12, pp. 3156-3167, 2010.
- [5] R. Pintelon, J. Schoukens, *System Identification: A Frequency Domain Approach*, 2nd ed., New Jersey: Wiley-IEEE Press, ISBN: 978-0470640371, 2012.
- [6] L. Ljung, *System identification: Theory for the User*, 2nd ed., New Jersey: Prentice-Hall, ISBN: 9780136566953, 1999.
- [7] P. Z. Csurcsia and J. Lataire, "Nonparametric Estimation of Time-variant Systems Using 2D Regularization," *IEEE Transactions on Instrumentation & Measurement*, vol. 65, no. 5, pp. 1259-1270, 2016.
- [8] P. Z. Csurcsia, "Static nonlinearity handling using best linear approximation: An introduction," *Pollack Periodica*, vol. 8, no. 1, 2013.
- [9] J. Schoukens, R. Pintelon, Y. Rolain, *Mastering System Identification in 100 exercises*, New Jersey: John Wiley & Sons, ISBN: 978047093698, 2012.
- [10] M. Solomou and D. Rees, "Measuring the best linear approximation of systems suffering nonlinear distortions: An alternative method," *IEEE Transactions on Instrumentation and Measurements*, vol. 52, no. 4, pp. 1114-1119, 2003.
- [11] T. Dobrowiecki and J. Schoukens, "Linear approximation of weakly nonlinear MIMO systems," *IEEE International Instrumentation and Measurement Technology Conference (I2MTC)*, pp. 1607-1612, 2004.
- [12] P. Guillaume, R. Pintelon, and J. Schoukens, "Accurate estimation of multivariable frequency response functions," *13th World Congress of IFAC*, vol. 29, no. 1, pp. 4351 - 4356, 1996.
- [13] R. Priemer, *Introductory Signal Processing*, World Scientific, ISBN: 9971509199, 1991.

- [14] M. Alvarez Blanco, P. Z. Csurcsia, K. Janssens, B. Peeters and W. Desmet, "Nonlinearity assessment of mimo electroacoustic systems on direct field environmental acoustic testing," in *International Conference on Noise and Vibration Engineering*, Leuven, 2018.
- [15] B. Peeters, M. El-Kafafy, P. Guillaume and H. Van der Auweraer, "Uncertainty propagation in Experimental Modal Analysis," in *Conference Proceedings of the Society for Experimental Mechanics Series*, 2014.